Marine Geology
January 2010, Volume 268, Issues 1-4, Pages 137-151
http://dx.doi.org/10.1016/j.margeo.2009.11.002

Buried fluvial incisions as a record of Middle–Late Miocene eustasy fall on the Armorican Shelf (Bay of Biscay, France)

Fabien Paquet[a, e, *], David Menier[a], Guilhem Estournès[a], Jean-François Bourillet[b], Pascal Leroy[c] and François Guillocheau[d]

[a] Université de Bretagne-Sud, EA 2219 GeoArchitecture, Campus de Tohannic — ENSIbs, rue Yves Mainguy, 56017 Vannes, France
[b] IFREMER, Centre de Brest, 29280 Plouzané, France
[c] IUEM, Technopôle Brest-Plouzané, 29280 Plouzané, France
[d] Université de Rennes 1, UMR-CNRS 6118 Géosciences Rennes, Campus de Beaulieu, CS 74205, F-35042 Rennes Cedex, France
[e] BRGM, Geology Division — Geology of Sedimentary Basins, 3 rue Guillemin, BP 36009, 45060 Orléans Cedex 2, France

*: Corresponding author : Fabien Paquet, Tel.: + 33 2 38 64 47 51; fax: + 33 2 38 64 33 33, email address : f.paquet@brgm.fr

Abstract:

High-resolution seismic data have been acquired in June 2008 on the Armorican Shelf (AS), in the northern Bay of Biscay, in order to reassess its stratigraphic architecture in detail and to study the impact of eustasy, tectonic and sediment delivery on the margin sedimentary record. Several profiles show fluvial-type incisions of several tens of meters (up to 54 m) associated to a widespread erosion surface. Several hypotheses are proposed for the stratigraphic position of this surface and incisions. We suggest Middle to Late Miocene age. Considering the relatively quiescent tectonic activity of the margin, we infer that the relative sea-level fall responsible of aerial incision on the Miocene shelf is eustasy-related. We propose the attested Serravallian–Tortonian eustatic lowstand (c. 11.6 Ma) as the key event responsible of such erosion and incision. This event marks the early beginning of the high-amplitude sea-level fluctuations that culminated during the Pleistocene and significantly controlled the present day AS morphology. The variability of vertical incision observed along single reaches can be explained by the confluence of several tributaries, the sinuosity of the channel and can be amplified by the unconsolidated nature of the Miocene substratum. The main pathways of the fluvial network corresponding to these buried valleys have been reconstructed and connections to other existing networks are proposed.

Keywords: Armorican Shelf; incised valleys; Miocene; eustasy; passive margin

1. Introduction

In low sedimentation rate and quiescent passive margins, eustasy has a predominant effect on the stratigraphic architecture ([Vail et al., 1977] and [Posamentier and Vail, 1988]). In such settings, the development of fluvial channel incisions over the shelf is considered as an indicator of a significant global sea-level fall and lowstand, that expose the entire shelf below or close to the breakpoint (Dalrymple et al., 1994) and is associated sometimes to submarine canyon incisions (Vail et al., 1991). Several examples are documented worldwide and are used to date or constrain the amplitude and effects of eustasy changes through time ([Fulthorpe et al., 1999], [Fulthorpe et al., 2000] and [Lofi and Berné, 2008]) or are the subject of ongoing studies (e.g. IODP expeditions 313 and 317). In the northern Bay of Biscay, numerous Quaternary incised valleys described over

the Armorican Shelf illustrate the impact of the high-amplitude Pleistocene glacio-eustasy falls (c. -120m) (Pinot, 1974; Menier et al., 2006; Chaumillon et al., 2008). Important sea-level falls of several tens of meters are also suspected for the Neogene period (Haq et al., 1987) and may have resulted in the generation of a fluvial networks over the emerged AS. Despite the presence of widespread erosion surfaces, related Neogene channel incisions are not attested and clearly described directly offshore southern Brittany. This is mainly due to the scarcity and the average quality of data (Bourillet et al., 2005). However, the "Quaternary" network drawn by Pinot (1974) was partly based on the detection of incisions on seismic data, c. 100 km from the present day coastline. Surprisingly, the Pleistocene valley network as described in recent studies (Menier, 2004; Menier et al., 2006; Thinon et al., 2008) does not extend that far over the outer shelf. A re-evaluation of the stratigraphic position of the outer-shelf incisions of Pinot (1974) was therefore needed to verify a pre-Quaternary age attribution. Evidence of potential Neogene channel incisions in surrounding areas is located in the Western Approaches and are associated with the 'Fleuve Manche' paleoriver system (Reynaud et al., 1999; Bourillet et al., 2006) where Neogene series are well-documented (Evans and Hughes, 1984), and to the South, over both the Vendean-Armorican Platform (Huerta et al., in press) and the North Aquitaine shelf (Bellec et al., 2009).

This study presents the interpretation of recent high-resolution seismic sparker profiles acquired on the Armorican Shelf that show clear incisions within the Miocene series. We discuss the origin and the age of these incised valleys, and describe their morphology and potential significance in terms of eustasy.

GEOLOGICAL SETTING

The Armorican Shelf (AS) corresponds to a segment of the European Atlantic margin in the northern Bay of Biscay (Fig .1). Its formation initiated during the Early Cretaceous (Barremian-Aptian, c. 125 Ma) consequently to the rotation of the Iberian Peninsula and the contemporaneous opening of the Bay of Biscay (Montardet et al., 1979; Olivet, 1996; Thinon, 1999). Its present day morphology corresponds to a large polygenetic erosion surface (wave-planed) resulting from significant Plio-Pleistocene sea-level fluctuations (Imbrie et al., 1984; Waelbroeck et al., 2002). The Cenozoic was dominated by post-rift mixed carbonaceous-silicoclastic sedimentation as revealed by exploration well PENMA-1 (Preux, 1978), and cores (Bouysse et al., 1974; Thomas, 1999; Guillocheau et al., 2003). The knowledge of the stratigraphic architecture of the AS is provided by interpretation of seismic data from the Bir Hakeim survey (Bouysse et al., 1968) and correlations with PENMA-1 well (Guillocheau et al., 2003). Post-rift deformation occurred mostly in response to the Pyrenean collision that reactivated strike-slip Variscan structures (Montardet et al., 1979). This subsequent Oligocene compressive phase did not affect obviously this area such as it did in the English Channel, with the modification of the Hurd deep (Lericolais et al., 2003). The limited Cenozoic tectonic activity in the study area is evidenced by sub-vertical faults that suggest a dextral strike-slip movement that faded during the Miocene (Fig. 4 and 5). The margin is also affected by an apparent seaward regional tilt documented onshore (Bonnet et al., 2000) and offshore (Vanney et al., 1972; Bourillet et al., 2003). Several regional erosion surfaces resulting from sea-level changes and/or phases of regional tilt are recorded and form angular unconformities (Fig. 1C, 4 and 5). One of these surfaces is interpreted to be middle to late Miocene in age (Vanney et al., 1972; Guillocheau et al., 2003, Bourillet et al., 2003). The

Miocene-recent deposits of the AS margin are mostly located on the median and outer parts of the shelf where they form a stack of wedges (Fig. 1C and 5). Incised valleys are present over the inner shelf and the coastal area (Boillot et al., 1971; Bouysse et al., 1974; Menier, 2003; Menier et al., 2006; Chaumillon et al., 2008). The origin of both these incisions and their valley fills is linked to Late Pleistocene sea-level fluctuations. Unfortunately, due to coarse superficial sediments, no attempts at coring have yet succeeded in recovering paleovalley fill (Bourillet and Turon, 2003).

Recently acquired high-resolution seismic data detail the geometry of the sedimentary succession and associated erosion surfaces. One of these surfaces revealed several incisions, c. 100 km from the present day coastline.

METHODOLOGY:

This study is based on the interpretation of high-resolution Sparker seismic data acquired onboard CNRS-INSU "Côtes de la Manche" vessel in June 2008 (GeoEtel-2008 survey,) as well as the re-interpretation of lower-resolution seismic profiles from older surveys (Bir Hakeim 1967, Job-ha-Zelian 1971, 1973 and 1974). Seismic units and bounding surfaces are defined by describing reflection continuity, amplitude, frequency, configuration and terminations (Mitchum et al., 1977a and 1977b). The seismic stratigraphy obtained from our interpretations have been geometrically correlated to cores and dredges samples and to PENMA-1 exploration well, which provides the only regional access to the Meso-Cenozoic sedimentary record (Fig. 5). These correlations have been made assuming a mean velocity of 2250 ± 250 $m.s^{-1}$ for the Miocene-recent interval and 2910 ± 10 $m.s^{-1}$ for the Oligocene one (velocity from Garlizenn-1 exploration well; Maillard, 1982).

RESULTS:

Seismic stratigraphy

Sparker seismic profiles image the sedimentary succession from Paleogene to Present from the median shelf to the shelf break. Six seismic units and one sub- unit have been identified (U1 to U6 and U6b) separated by six bounding surfaces (S1 to S6). Seismic characteristics of units and surfaces are described in Table 1. Each unit is composed of one seismic facies that does not vary significantly laterally. In the following section, we describe the seismic stratigraphy in terms of geometry and stacking pattern. We also propose both lithology and stratigraphic position for units when they are documented by subsurface samples, by correlations to surfaces at PENMA-1 well (Preux, 1978), and on the basis of former studies (*e.g.* Vanney et al., 1972; Guillocheau et al., 2003).

Seismic unit 1 (U1):

U1 is the lower most unit identified on seismic data. As a result, no basal boundary is visible on seismic data. Its seismic facies shows chaotic and locally steep reflections (Table 1). It crops out along the present day coastline where it as been sampled (Fig. 5). It consists of metamorphic (micaschists) and crystalline (granites) Paleozoic rocks deformed during the Variscan orogeny (Audren and Lefort, 1977). It therefore forms the basement of the AS. The upper boundary of U1 is a clear erosion surface (S1) and represents the base of the sedimentary succession of the AS.

Seismic unit 2 (U2):

U2 lies directly on the Variscan basement where it presents few onlap terminations on S1. Its thickness is unclear but probably exceeds 400 ms (Fig. 5). U2 is made up of parallel and continuous reflections (Table 1) characteristic of well-bedded marine sediments. U2 is sampled in PENMA-1 and at several locations over the inner shelf where it corresponds to Paleogene chalks, calcareous mudstones and sandstones with rare terrigeneous-rich beds (Andreieff et al., 1968; Barbaroux et al., 1971; Bouysse et al., 1974; Delanoë and Pinot, 1974; Delanoë et al., 1975; Preux, 1978). U2 is bounded above by erosion surface S2 highlighted by toplap terminations (Fig. 4 and 5) that reflects a slight regional tilt (< 0.5°). U2 is affected by brittle deformation with NW trending sub-vertical faults and gentle folds (Fig. 1, 4 and 5).

The presence of the thick Cretaceous section (c. 500 m) identified in the lower third of PENMA-1 (Fig. 3) is not attested at the seafloor, over the inner shelf, between basement and U2. This may be due to a landward thinning and/or onlap of the series as visible in petroleum conventional seismic data (unpublished petroleum data).

Seismic unit 3 (U3):

U3 is a 40-50 ms-thick unit characterized by discontinuous and slightly wavy very high-amplitude reflections (Table 1). It is bounded below by unconformity S2 and above by S3 that shows rather little erosion except on line 20-670 (Fig. 5). No seafloor samples have been collected in the area where the unit may crops out. Nevertheless, U3 correlates geometrically to the upper-part of the Oligocene series (Chattian?) at PENMA-1 (Fig. 5) where it is made up of shallow marine coral-rich bioclastic sandstones (Fig. 3). Discontinuity and wavy forms of reflections within U3 may correspond to small coral reefs or mounds. The mapping extent of U3 is unclear but should consist in a narrow corridor seaward from U2. Tectonic deformation style

affecting U3 is similar to U2 but in an evident lesser proportion (Fig. 4 and 5). This observation and the tilting of U2 suggest that a deformation phase occurred during Paleogene with a probable culmination between Late Eocene and Late Oligocene. Such a phase is described by several regional studies and syntheses and corresponds to the Pyrenean compressive tectonic phase *s.l.* (Gély and Sztràkos, 2001). It is supposedly responsible for 1) the inversion in the English Channel documented between the Mid-Late Eocene and Early-Oligocene (Ziegler, 1987; Evans, 1990), 2) the sedimentary hiatus in the Bay of Biscay (Hailwood et al., 1979), and coincides with the contemporaneous uplift of North Atlantic margins (Anell et al., 2009 and references herein). This phase may have partly triggered the development of S2 unconformity.

Seismic unit 4 (U4):

U4 is a 100 to 150 ms-thick unit made up of sub-parallel, continuous and low-amplitude reflections (Table 1). It shows downlap terminations on its lower boundary S3 and an overall progradation pattern interrupted by transgressive phases of a lesser order evidenced by onlap surfaces (Fig. 4 and 5). The seismic facies suggest well-bedded fine grained deposits (mudstones, siltstones). U4 is topped by a widespread erosion unconformity that is characterized by toplap terminations of the underlying reflections (Fig. 4 and 5). This erosion surface is more or less penetrative into the underlying sediments and locally shows clear deep incisions on several profiles (Fig. 4, 5 and 6). Very few seafloor samples have been collected in the area (Fig. 1) and mainly consist in Miocene calcareous marls and Aquitanian bioclastic limestones (Andreieff et al., 1968). At PENMA-1, S3 and the lower part of U4 respectively correlate with a thin poorly-sorted terrigeneous sandstone bed and a Miocene mixed marine terrigeneous-calcareous mudstone. This unit may find lateral equivalents in

190 the Miocene –faluns" (shallow marine mixed bioclastic and terrigeneous coarse sands)
191 that are well documented onshore (Brittany, Anjou, and Tourraine areas; Lécuyer et
192 al., 1996; Néraudeau, 2003)

193 These observations suggest that S3 developed at the transition between a documented
194 Oligocene sea level low and a Miocene sea level high (Haq et al., 1987) evidenced by
195 the change from shallow marine limestones with corals to transgressive glauconitic
196 sandstone then prograding marine mudstones (Preux, 1978). The upper part of U4 is
197 not sampled or described in PENMA-1 (no recovery), it is thus lacking reliable
198 lithology and age calibrations (see discussion). The upper limit S4 presents evident
199 erosion features including irregular toplap/truncation surface with channel-like
200 incisions (Fig. 4, 5 and 6). As for S2, the toplap terminations evidenced a slight
201 seaward tilt (< 0.5°) of the sedimentary section (Fig. 5). The age calibration of S4 can
202 not be directly determined from existing samples and different hypotheses are
203 addressed in the discussion section.

204 **Buried channel incisions of S4**

205 Among several unconformities identified in the seismic stratigraphy of the AS, S4 is
206 the oldest to exhibit a deeply incised surface. Careful study of available seismic
207 profiles allows a better understanding of the processes resulting in the generation of
208 S4 and associated erosion features (Fig. 4 and 6). Incisions present (1) major and
209 deeper channels with (2) several associated secondary channels (tributaries), separated
210 by (3) strath terraces developing in (4) a wider valley. These observations are in
211 agreement with a fluvial and thus subaerial origin for the incisions (Posamentier,
212 2001). A possible karstic origin for these features is neglected here because the
213 incised lithologies contain a terrigeneous fraction (PENMA-1, Preux, 1978). The

214 incision depth of the major channel and the valley shape along transversal profiles
215 vary dramatically (Fig. 6). On profiles 7 and 26 (Fig. 6a and 6c), the vertical incision,
216 from the valley edges to the channel bottom, reaches 30 ms and 60 ms respectively
217 (30 m and 60 m at 2000 $m.s^{-1}$) and is strongly localized, whereas, in between, on
218 profile 22, incision is less deep (10 ms; 10 m at 2000 $m.s^{-1}$) (Fig. 6b). Likewise, the
219 shape of channels on seismic profile shows a clear variability from V-shape (e.g.
220 Profile 26, Fig. 6a) to U-shape (e.g. Profile 7, Fig. 6c) with more or less symmetry.
221 This is in agreement with seismic profiles crossing sinuous valley reaches with
222 variable azimuth angles (Fulthorpe et al., 1999). The density of seismic profiles
223 allows the mapping of a paleo-fluvial network in that area (Fig. 7 and 8). We
224 tentatively trace four distinct valleys, labeled A, B, C and D, from west to east, by
225 correlating incisions between profiles (Fig. 8). Valleys strike to the NE-SW,
226 orthogonally to the margin. As incision depth fades seaward and as S4 and associated
227 valleys are eroded landward by S6, the network can not be traced over more than 30-
228 40 km (Fig. 8). Our interpretations suggest a connection of both valleys B and C
229 downstream. The valley fill deposits (base of U5) are made up of several sub-units
230 separated by U-shaped erosion surfaces that laterally incise and widen the preexisting
231 main channel (e.g. profile 26, Fig. 6a). On profile 7, younger channelized incisions
232 are visible and one of them truncates the main erosion surface S4 (Fig. 6c). Therefore,
233 generation and reshaping of S4 erosion surface ends after deposition of U5 starts.

234 Seismic unit 5 (U5):

235 U5 is a 40-50 ms-thick lens-shaped unit that thins both landward and seaward (Fig. 5).
236 It shows very chaotic and discontinuous reflections with channels and onlap
237 terminations on S4 (Table 1). Such seismic facies suggests sandy sediments. Deposits
238 in the basal part of U5 fill the S4 incisions and present U-shaped erosion surfaces that

239 locally incise U4. Above, the upper-boundary S5 shows unusual characteristics with
240 possible channel incisions (Fig. 4 and 5) and a seaward truncation of several U5
241 reflections (Fig. 5). The age of U5 is not defined as but intersection between S5 and
242 sea floor corresponds to the base of the Pliocene-Pleistocene sedimentary succession.

243 Seismic Unit 6 (U6):

244 U6 is a >200 ms-thick unit that corresponds to the seaward most seismic unit
245 individualized in this study. It lies conformably over S5 and reflections are
246 discontinuous, chaotic with possible channels (Table 1) and show a seaward dip of c.
247 5° (Fig. 5). The seismic facies is similar to U5 suggesting sandy material. The upper
248 boundary of U6 corresponds to the "flat" sea floor that forms the morphology of the
249 shelf. U6, as well as all the other seismic units (U1 to U5) is strongly eroded at the sea
250 floor. On GeoEtel-2008 seismic data (eg. Fig. 4, 5 and 6), this erosion surface is
251 resolved as 1) a proper erosion surface topped by 2) a thin and discontinuous sediment
252 cover (sub-unit U6b). This sediment cover is made up of unconsolidated mixed
253 terrigeneous and bioclastic clayey sands of Holocene age. The age calibration of U6
254 can not be attested with certainty as no sea floor sample exists in the area except for
255 U6b. Nevertheless, U6 being the last and thus youngest unit of the AS we propose a
256 Pliocene-Pleistocene age. This is also supported by the complex internal stacking
257 pattern with several unconformities that may illustrate the impact of the Plio-
258 Pleistocene eustasy variations. S6 may therefore correspond to the last member of a
259 series of coincident erosion surfaces resulting from the dramatic high-amplitude
260 Pleistocene sea level variations.

261

262 **Summary:**

263 Our seismic interpretation allows the identification of six seismic units separated by
264 major unconformities. The first unit U1 corresponds to the Paleozoic basement and
265 the following ones represents the Cenozoic sedimentary cover of the Armorican Shelf.
266 Lithology, calibrated from core samples and PENMA-1 well progressively evolves
267 from a biogenic carbonate-dominated sedimentation to mixed bioclastic-terrigeneous
268 deposits throughout the whole sediment section. Several unconformities show erosion
269 features and both S2 and S4 record phases of Cenozoic seaward tilting of the margin.
270 S4 is the oldest erosion surface to exhibit deeply incised fluvial valleys. It seems to
271 mark an important step in the transition between the two sedimentation styles stated
272 above. In the following section we discuss the age calibration of S4, the deciphering
273 of the various controlling parameters that lead to its generation, the morphology of the
274 valley reaches, and its significance in terms of paleogeography and evolution of the
275 shelf morphology.

276

277 **DISCUSSION:**

278 Existence of fluvial channels on the AS continental margin indicates that rivers were
279 once flowing over the emerged shelf but the stratigraphic position of the incised
280 erosion surface S4 within sedimentary succession is still unclear. These channel-like
281 incisions had already been described by Pinot (1974) and associated to a continuous
282 late Pliocene-Pleistocene fluvial network extending over the AS and connecting
283 onshore valleys to the slope canyons. Nevertheless, careful study at the newly
284 acquired seismic data reveals that 1) the channels are associated with the tilted
285 Neogene S4 erosion surface and that 2) no direct connections to the inner shelf
286 paleovalleys and/or slope canyons can be traced.

287 **Age calibration of S4:**

288 Seismic units (U4 and U5) on both side of S4 have not been properly dated making
289 age calibration of this surface rather speculative. Our interpretation and correlations
290 to PENMA-1 indicate that U3 and the base of U4 are of Late Oligocene and Early
291 Miocene age respectively, and that a Pliocene-Pleistocene age is confidently
292 attributed to U6. Therefore, the age of S4 is comprised between Early Miocene and at
293 some stage in Pliocene. By analogy to the documented stratigraphy of the nearby
294 Western Approaches (Fig. 9) where incised valleys are also identified (Evans and
295 Hughes, 1984; Powell, 1988; Reynaud et al., 1999, Bourillet et al., 2003; Stewart and
296 Davies, 2007), two hypotheses can be formulated as follow. These hypotheses are
297 then tested using the event timing of regional and global controlling parameters
298 (tectonic deformation, eustasy, and climate) that have been recorded in Western
299 Europe and in other remote margins.

300 ***Hypothesis 1 – "Late Miocene-Pliocene" age model:***

301 In this model, 1) U4 is the lateral equivalent of both Jones and Cockburn formations
302 that are of early to mid-Miocene (Aquitanian-Serravallian) and of mid- to late
303 Miocene age respectively (Evans and Hughes, 1984; Powell, 1988), and 2) U5 and
304 U6-U6b correspond to both the Plio-Pleistocene Little Sole formation and the
305 Pleistocene-Holocene Melville formation respectively. In such context, S4 and
306 associated valleys are likely of late Miocene - Pliocene age. This is in agreement with
307 both the Messinian age preferred by Bourillet et al. (2003) and the late Pliocene age
308 proposed by Reynaud et al. (1999) for the lateral equivalent of S4 in the Western
309 Approaches.

310 ***Hypothesis 2 – "Mid-Late Miocene" age model:***

311 In this model, U4 has only the Jones formation as lateral equivalent whereas the
312 Cockburn formation correlates with U5, and both U6 and U6b are equivalent to the
313 Little Sole and the Melville formations. Thus S4 developed earlier, close to the mid-
314 late Miocene boundary. Such an attribution is also consistent with the study of
315 Bourillet et al. (2003) that indeed proposed an age ranging from c. 12 Ma
316 (Serravallian-Tortonian) to c. 5 Ma (Messinian). Late-Pliocene incised valleys
317 (Reynaud et al., 1999) would find more suitable equivalents within U6 where
318 channels are described.

319 Without reliable ages, discussing S4 age models requires to determine the possible
320 control parameters that lead to S4 development and the related timing of events.
321 Fluvial incisions into marine deposits evidence the emergence of the shelf that implies
322 an important relative sea-level (base-level) fall. Such a fall find its origin in either (1)
323 a tectonic deformation (local uplift) and/or (2) an eustatic fall (global).

324 **Cenozoic tectonics:**

325 Tectonic deformation within the sedimentary succession of the AS and identified on
326 seismic data is characterized by sub-vertical faults and associated folds that affect
327 mostly the seismic unit U2 (Paleocene-Eocene). Angular unconformity S2 seals most
328 of the brittle deformation and only few faults traverse the following seismic units
329 (Fig. 4 and 5). S4 corresponds to another angular unconformity that shares several
330 features with S2, including toplap terminations of U4 reflections.

331 Over the Bay of Biscay area and over the AS, the Cenozoic tectonic deformation is
332 attributed to the alpine orogeny *s.l.* (Fig. 9). Two major phases are recognized in the
333 literature (Ziegler, 1990; Bourrouilh et al., 1995). The Pyrenean phase *s.l.* extends
334 from Eocene to mid-Oligocene (Gély and Sztràkos, 2000 and 2001). It is expressed on

335 the AS as the series of sub-vertical faults (reactivated Variscan structures) and folds
336 visible in the contemporaneous seismic unit U2 (Bouysse et Horn, 1971; Delanoë,
337 1988), and as the Oligocene angular unconformity S2 that mostly seals this
338 deformation (Fig. 4 and 5). Contemporaneously with the late Pyrenean phase is the
339 first basin inversion of the Western Approaches Trough (Ziegler, 1987). The second
340 phase of deformation is related to the Miocene Alpine contractional phase. Its record
341 on the AS may correspond to the play of part of the Paleogene sub-vertical faults that
342 affect seismic units from U3 to U6 (Oligocene to recent). Similarly to S2, erosion
343 surface S4 is an angular unconformity that also highlights and seals a Neogene tilt of
344 the AS toward the SW (Fig. 4 and 5). This phase is also contemporaneous with a new
345 phase of inversion in the Western Approaches Trough, and both are of mid-late
346 Miocene to Pliocene age (Ziegler, 1987, 1990, Guillocheau et al., 2000). Thus,
347 Neogene tectonic deformation phases provide a good framework to explain the
348 various features identified on seismic data. Unfortunately, the duration of these phases
349 and the poor age control on their pulses preclude any accurate age calibration of S4.
350 Alternatively, northwest European passive margins undergone both tilting and
351 sagging attributed to mantle-driven processes during Cenozoic (Praeg et al., 2005) but
352 the timing and signature of deformation differs from what is recorded along the AS.
353 Finally, looking at the present day architecture of the AS margin (Fig. 4), the angular
354 erosion unconformity S6 attests a Plio-Pleistocene tilt of the margin that has increased
355 the subsidence of the outer shelf and the burial and preservation of S4 incised valleys.

356 **Cenozoic eustasy:**

357 During Cenozoic, sea level has undergone important and abrupt changes (Fig. 9)
358 accompanying the overall transition from the Mesozoic early-Cenozoic greenhouse to
359 the Quaternary icehouse conditions (Haq et al., 1987; 1988; Miller et al., 1998; Miller

et al., 2005). One example is the postulated mid-Oligocene eustatic lowstand visible on the eustatic curve of Haq et al. (1987; 1988) close to the Rupelian-Chattian boundary, or alternatively attributed to an earlier Oligocene cooling event by Miller et al. (2008). According to different studies the estimated amplitude of the fall varies from -160 m (Haq et al., 1987) to -55 m (Miller et al., 2005). On the AS, this documented early- or mid-Oligocene eustatic fall correlates fairly well with the S2 erosion unconformity and is also illustrated by the transition from the outer-shelf Eocene marine deposits from shallower inner-shelf Oligocene deposits described at PENMA-1 (Preux, 1978; Guillocheau et al., 2003) (Fig. 3). Thus, the generation of S2 unconformity and its characteristics would result from the combined effects of both tectonic deformation and a eustatic sea level fall.

Considering the similarity between S2 and S4 unconformities (Fig. 5), and especially the existence of incised fluvial valleys (Fig. 4, 5 and 6), the generation of S4 would have required a relative sea level fall following the Oligocene fall event with amplitude similar or greater. One other major climatically-induced sea level fall documented worldwide for this period starts during the late Langhian - early Serravallian (c. 14 Ma) and culminates around the Serravallian-Tortonian boundary (mid-late Miocene boundary at 11.608 Ma – GSSP; Hilgen et al., 2005) (Haq et al., 1987, 1988; Kominz et al., 1998; Miller et al., 1998; John et al., 2004; Miller et al., 2005). The Serravallian-Tortonian boundary correlates to the glacio-eustatic lowstand T3.1 (Haq et al., 1987, 1988) associated with the permanent establishment of the East Antarctic Ice Sheet (Zachos et al., 2001). The amplitude of the Middle Miocene sea-level fall estimated in former studies is still debated with values ranging from -25 m to -180 m (Haq et al., 1987; Pigram et al., 1992; Miller et al., 1998; John et al., 2004). We propose that S4 and associated channel incisions were completed close to the

385 Serravallian-Tortonian boundary at c. 11.6 Ma with a probable initiation occurring
386 earlier during late-Langhian early-Serravallian. The onset of the Icehouse and long-
387 term sea-level lowstand conditions would also explain the presence of several
388 younger (e.g. Tortonian and Messinian) channelized erosion surfaces identified within
389 U5 and U6 (Fig. 4 and 5). In addition, Mio-Pliocene fluvial network remnants have
390 been described onshore in Brittany (Guillocheau et al., 1998; Van Vliet-Lanoë et al.,
391 1998) in several places including Lauzach and Réguigny (Fig. 8). The basal fluvial
392 deposits filling the oldest incised valleys have been dated by ESR at 8.7 ± 1.5 Ma
393 within the Tortonian (Van Vliet-Lanoë et al., 1998; Brault et al., 2004). This suggests
394 a possible Serravallian or early-Tortonian age for the incision phase. The
395 reconstruction of the Tortonian network provided by Brault et al. (2004) and based on
396 paleocurrent directions shows a southwestward direction for both the onshore
397 Tortonian and the supposedly contemporaneous offshore S4 fluvial networks (Fig. 7).
398 In addition, onshore outcrops exhibit several erosion surfaces and associated fluvial
399 networks (Brault et al., 2004). This configuration is shared by the offshore buried
400 valleys that show several younger incisions (Fig. 6). Thus, both offshore and onshore
401 networks could be genetically linked. Unfortunately, due to the joint effects of (1) the
402 Neogene seaward regional tilting of the AS and (2) the wave abrasion that occurred
403 during the Plio-Pleistocene sea-level fluctuations and gave its shape to the present day
404 AS (polygenetic wave-planed surface), the channelized erosion surface is only
405 preserved 100 km offshore the present day coastline. Such configuration avoids direct
406 correlations between this distal buried fluvial network and the onshore one. In the
407 same way, the question could be asked about the age of the so-called Quaternary
408 inner-shelf incised valleys. If a Plio-Pleistocene age for the sedimentary fill sounds

409 reasonable (Menier et al., 2006; Proust et al., 2009), the incision phase could be
410 underestimated (Menier, 2004) and be reassessed to the mid-Miocene time.

411 Compared to surrounding areas, a Serravallian-Tortonian boundary age attribution for
412 S4 seems reasonable. Over the North Aquitaine Shelf, Bellec et al. (2009) describe
413 several unconformities showing incised valleys. They propose that these surfaces
414 formed during the successive Langhian to early-Tortonian sea level falls, the last one
415 being the most erosive and correlating T3.1 sea level fall of Haq et al. (1987) as
416 proposed for S4 on the AS. The absence of earlier incisions below S4, within U4, may
417 be explained by (1) lower subsidence and sedimentation rates of the AS area that
418 resulted in the stacking of all surfaces in only one (S4) or (2) because incisions
419 occurred landward and have been eroded later (Fig. 5). Over the Western Approaches,
420 the age of the incised valleys is still debated but Bourillet et al. (2003) propose an age
421 ranging from 12 to 5 Ma (Serravallian to Messinian) based on a range of subsidence
422 rates. Such an age range is compatible with our age estimation for S4. Likewise,
423 major erosion unconformities attributed to mid- to late Miocene sea level falls are
424 described in other remote passive margins such as the New Jersey shelf (Fulthorpe et
425 al., 1999), the northern Java shelf (Posamentier, 2001), and the Gulf of Lions (Besson
426 et al., 2005). The sea level fall at the Serravallian-Tortonian boundary is specifically
427 preferred as the triggering event for several of these surfaces such as in the Gulf of
428 Papua (Tcherepanov et al., 2008) or in the Gulf of Lions (Lofi and Berné, 2008).

429 We thus favor the second hypothesis, and consequently attribute a Tortonian age to
430 U5 (equivalent of the WA Cockburn formation and the first onshore ~~–R~~ed Sands"
431 (Fig. 9). Erosion surface S5 could be of Messinian or basal Pliocene age (Haq events
432 TB3.4 or 3.6). U6 would therefore correspond to the Pliocene-Pleistocene outer shelf
433 sedimentary prism and is a lateral equivalent of the Little Sole formation.

434 The Serravallian eustatic fall would have thus progressively exposed the shelf of the
435 AS, thus creating the major unconformity S4 and associated channels. This event took
436 place while the whole AS undergone a regional tilt related to the Alpine orogenic
437 phase. It results that S4 developed also as an angular unconformity. This tilt has
438 induced a local uplift of the area thus increasing the effect of eustasy on the relative
439 sea level fall, and enhancing the stratigraphic signature S4.

440 **Significance of the valley morphology**

441 At its lowest, the Serravallian – Tortonian sea level may have reached depth close to
442 or even below the smooth and rounded clinoform breakpoint. Potential connection
443 between S4 incised valleys and hypothetical mid-Miocene slope canyons, is not yet
444 demonstrated. This is mainly due to the scarcity of data and their rather low
445 penetration where the mid-late-Miocene strata are buried below the thick Plio-
446 Pleistocene wedge. Nevertheless, when looking at the vertical incision depth of the
447 four valleys, it tends to decrease south-westward (seaward) indicating that valleys and
448 canyons are not directly connected.

449 Alternatively, depth of vertical fluvial incision on shelves is often considered as a
450 proxy for estimating the depth reached during the sea-level lowstand. Concerning the
451 valleys described in this study, the use of the depth of channels, to estimate the
452 contemporaneous sea-level appears problematic. The observed variability of depth
453 incision of one valley between seismic sections corresponds to large-scale undulations
454 of the river bottom longitudinal profile and suggests a riffle-pool sequence
455 morphology developing on a sinuous channel (Richards, 1982; Lofthouse and Robert,
456 2008). Testing this hypothesis would require additional data in order to constrain the
457 three-dimensional morphology of the channels, the length of the riffle-pool sequence,

458 and finally, to discuss the potential river characteristics (e.g. water discharge,
459 sediment load, grain-size). The ―pool" areas may also be controlled by the confluence
460 of one or more tributaries with the main channel. In addition, we consider that the
461 young and unconsolidated lower to middle Miocene series, incised by the Mid-
462 Miocene rivers, has played a significant role by facilitating the incision in the ―pools"
463 areas. Such variability of the depth of incision thus precludes accurate and reliable
464 estimation of the depth reached by the sea-level during the late Serravallian – early
465 Tortonian lowstand. Moreover, the tectonic tilt of the margin and the associated uplift
466 of the area, evidenced by the angular unconformity S4, have also played a role in the
467 relative amplitude of the sea-level fall. Additional data are needed to better
468 understand the valley morphology and its relation with the shelf edge.

469

470 **CONLUSIONS**

471 High-resolution seismic data recently acquired on the Armorican Shelf reveals the
472 presence of buried channel incisions developed on a widespread erosion surface S4, c.
473 100 km from the present day coastline. Reconstruction of the paleo-fluvial network
474 reveals the sinuosity of the valleys and the potential riffle-pool morphology. These
475 incisions are the same described by Pinot (1974) but considering their stratigraphic
476 position, a Quaternary age is unlikely. Based on the seismic interpretation of the AS
477 stratigraphy, correlation to the eustatic sea-level curve of Haq et al. (1987), and from
478 comparison to other margins, we propose that the unconformity S4 is rather of mid-
479 Neogene age. We also assume that the relative sea-level fall required for creating
480 such fluvial incisions on an exposed shelf was predominantly controlled by eustasy.
481 As an angular unconformity, S4 developed contemporaneously with a tilting of the

482 margin related to the Miocene Alpine orogenic phase. The associated uplift may have
483 increased the relative sea-level fall in the area, thus favoring the emersion of the shelf.
484 The most suitable eustatic fall event in terms of timing and amplitude initiated in the
485 Serravallian and culminated at the Serravallian-Tortonian boundary. Therefore we
486 proposed an age of c. 11.6 Ma for the completion of these incisions. Such an
487 attribution needs to be validated by new samples as other potential ages are proposed
488 in other studies for surrounding analogues. These valleys correlate well in both age
489 and direction with mid-Miocene incised valleys described onshore, over Brittany. The
490 question remains on the age of the incision phase of the inner shelf Quaternary incised
491 valleys. This improves our knowledge of the local Miocene paleogeography. Together
492 with recent results on the North Aquitaine shelf, these results provide new arguments
493 that tend to confirm the significance of the eustatic fall at the Serravallian-Tortonian
494 transition and its record on the northern margin of the Bay of Biscay. The expression
495 of the Serravallian-Tortonian boundary on the AS margin marks the beginning of high
496 amplitude eustatic fluctuations (icehouse) culminating during Pleistocene and creating
497 its present day plateau morphology (polygenetic wave-planed surface). The variation
498 in the depth of incision characteristic of riffle-pool morphology limits the ability to
499 quantify the relative and/or absolute sea-level fall. We finally point out that the
500 detailed knowledge of the valley three-dimensional morphology (riffle-pool,
501 meander) is requested before interpreting the significance of the incision depth in
502 terms of local and global controls. Additional data acquisition and interpretation are
503 requested to better constrain the geometry of the network and the relationship with the
504 shelf edge and potential interactions with Miocene slope canyons.

505 **ACKNOWLEGMENTS:** This study has been funded by société Lafarge and by the
506 Université de Bretagne-Sud, within the framework of the PERI-ARMOR project,

(Chief scientist: Dr. David Menier). The authors would like to thank Craig Fulthorpe and an anonymous reviewer for their pertinent comments on the earlier versions of the manuscript. The seismic acquisition material has been provided by the University of Rennes 1 – Géosciences Rennes (Dr. Jean-Noël Proust). The authors also wish to thank Alexandre Dubois, Florent Scalliet, and Camille Traini for their collaboration, discussions, and assistance during the GeoEtel-2008 survey. We are also indebted to the crewmembers of the CNRS-INSU vessel ―Côte de la Manche".

REFERENCES:

Andreieff, P., Bouysse, P., Horn, R., L'Homer, A., 1968. Données récentes sur l'Eocène au large de la Bretagne méridionale. Compte Rendu Sommaire des Séances de la Société Géologique de France, v. 5, 161-162.

Anell, I., Thybo, H., Artemieva, I.M., 2009. Cenozoic uplift and subsidence in the North Atlantic region: Geological evidence revisited. Tectonophysics. 474, 78-105.

Audrun, C., Lefort, J-P., 1977. Géologie du plateau continental sud armoricain entre les îles de Glénan et de Noirmoutier. Implications géodynamiques. Bulletin de la Société Géologique de France. 7, 395-404.

Barbaroux, L., Blondeau, A., Margerel, J-P., 1971. Présence d'Yprésien fossilifère sur le plateau continental à l'Ouest du plateau du Four (Loire-Atlantique). Comptes Rendus de l'Académie des Sciences. 273, 12-15.

529

530

531 Bellec, V.K., Cirac, P., Faugères, J-C., 2009. Formation and evolution of paleo-
532 valleys linked to a subsiding canyon, North Aquitaine shelf (France). Comptes
533 Rendus de l'Académie des Sciences, Paris, doi:10.1016/j.crte.2008.07.016.

534

535 Besson, D., Parize, O., Rubino, J-L., Aguilar, J-P., Aubry, M-P., Beaudoin, B.,
536 Berggren, W.A., Clauzon, G., Crumeyrolle, P., Dexcote, Y., Fiet, N., Iaccarino, S.,
537 Jime´nez-Moreno, G., Laporte-Galaa, C., Michaux, J., Von Salis, K., Suc, J-P.,
538 Reynaud, J-Y., Wernli, R., 2005. Latest Burdigalian network of fluvial valleys in
539 southeast France (western Alps), characteristics, geographic extent, age, implications:
540 Comptes Rendus Geosciences, 337, 1045–1054.

541

542 Boillot, G., Bouysse, P., Lamboy, M., 1971. Morphology, sediments and Quaternary
543 history of the continental shelf between the Straits of Dover and Cape Finisterre.
544 ICSU/SCOR Working Party 31 Symposium. Cambridge, U.K. In: Delay, F.M. (Ed.),
545 The Geology of the East Atlantic Continental Margin, Institute of Geological
546 Sciences. 70, 75–90.

547

548 Bonnet, S., Guillocheau, F., Brun, J-P., Van Den Driessche, J., 2000. Large-scale
549 relief development related to Quaternary tectonic uplift of a Proterozoic– Paleozoic

550 basement: the Armorican Massif, NW France. Journal of Geophysical Research. 105,
551 19,273–19,288.

552

553 Bourillet, J-F., Reynaud, J-Y., Baltzer, A., Zaragosi, S., 2003. The _Fleuve Manche‘:
554 the submarine sedimentary features from the outer shelf to the deep-sea fans. Journal
555 of Quaternary Science. 18, 261–282.

556

557 Bourillet, J-F., Turon, J-L., 2003. Rapport scientifique de la mission
558 MD133/SEDICAR. Les rapports de campagne à la mer, IPEV, Brest, OCE/2003/04,
559 150 pp.

560

561 Bourillet, J-F., Menier, D., Gaborit, K., 2005. Architecture des sédiments quaternaires
562 et vallées incises de la marge sud-armoricaine. In: Abstract Volume 10ème Congrès
563 Français de Sédimentologie. ASF, Paris, Presqu‘île de Giens, 11-13 October 2005,.
564 42.

565

566 Bourillet, J-F., Zaragosi, S., Mulder, T., 2006. The French Atlantic margin and the
567 deep sea submarine systems. Geo-Marine Letters. 26, 311-315.

568

569 Bourrouilh, R., Richert, J-P., Zolnaï, G., 1995. The North Pyrenean Aquitaine basin,
570 France: evolution and hydrocarbons. AAPG Bulletin. 79, 831–853.)

571

572 Bouysse, P., Horn, R., 1971. Etude structurale du plateau continental au large des
573 côtes méridionales de la Bretagne. Cahiers Océanographiques. 23, 497-517.

574

575 Bouysse, P., Horn, R., Le Gorgeu, J-P., 1968. Résultats d'une prospection sismique
576 réflexion continue en Bretagne méridionale, entre Penmac'h et Belle-Île. Comptes
577 Rendus de l'Académie des Sciences, Paris. 267, 568-571.

578

579 Bouysse, P., Chateauneuf, J-J., Ters, M., 1974. Présence d'Yprésien, niveau
580 transgressif et taux de sédimentation flandriens en baie de Vilaine (Bretagne
581 méridionale). Comptes Rendus de l'Académie des Sciences, Paris. 279, 1421-1424.

582

583 Brault, N., Bourquin, S., Guillocheau, F., Dabard, M-P., Bonnet, S., Courville, P.,
584 Estéoule-Choux, J., Stepanoff, F., 2004. Mio–Pliocene to Pleistocene
585 paleotopographic evolution of Brittany (France) from a sequence stratigraphic
586 analysis: relative influence of tectonics and climate. Sedimentary Geology. 163, 175-
587 210.

588

589 Chantraine, J., Autran, A., Cavelier, C. and others, 1996. Carte géologique de la
590 France à 1/1 000 000, Revised 2003. Editions BRGM, Orléans.

591

592 Chaumillon, E., Proust, J-N., Menier, D., Weber, N., 2008. Incised-valley
593 morphologies and sedimentary-fills within the inner shelf of the Bay of Biscay
594 (France): A synthesis. Journal of Marine Systems. 72, 383-396.

595

596 Dalrymple, R.W., Boyd, R., Zaitlin, B. R., 1994. History of research, types and
597 internal organization of incised-valley systems: Introduction to the volume, *in*
598 Dalrymple, R.W., et al., eds., Incised-valley systems: Origins and sedimentary
599 sequences. SEPM (Society for Sedimentary Geology) Special Publication. 51, 3–10.

600

601 Delanoë, Y., 1988. Les grands traits de la structure et de l'évolution géodynamique
602 des dépôts tertiaires du plateau continental sud-armoricain d'après les enregistrements
603 de sismique réflexion. Géologie de la France. 1988-1, 79-90.

604

605 Delanoë, Y., Pinot, J-P., 1974. Etude structurale du Tertiaire de la région du Banc
606 Bertin entre Belle-Ile et les Iles de Glénan (Bretagne méridionale). Union des
607 Océanographes de France. 6, 59-65.

608

609 Delanoë, Y., Lehébel, L., Margerel, J-P., Pinot, J-P., 1975. La Baie de Concarneau est
610 un bassin tectonique dans lequel d'épais dépôts du Lutétien supérieur ont été
611 conserves. Comptes Rendus de l'Académie des Sciences. 281, 1947-1950.

612

613 Delanoë, Y., Margerel, J-P., Pinot, J-P., 1976. En Baie de Concarneau, l'Oligocène
614 marin est discordant sur un Eocène ondulé, faillé et érodé, et l'Aquitanien a voilé
615 l'ensemble après une nouvelle pénéplanation. Comptes Rendus de l'Académie des
616 Sciences. Paris. 282, 29-32

617

618 Evans, C.D.R., 1990. United Kingdom Offshore Regional Report: the Geology of the
619 Western English Channel and its Western Approaches. British Geological Survey,
620 NERC, HMSO: London.

621

622 Evans, C.D.R., Hughes, M.J., 1984. The Neogene succession of the South Western
623 Approaches, Great-Britain. Journal of the Geological Society of London, 141(2), 315-
624 326.

625

626 Fulthorpe, C.S., Austin, J.A., Jr., Mountain, G.S., 1999. Buried fluvial channels off
627 New Jersey: Did sea-level lowstands expose the entire shelf during the Miocene?.
628 Geology. 27, 203–206.

629

630 Fulthorpe, C.S., Austin, J.A., Jr., Mountain, G.S., 2000. Morphology and distribution
631 of Miocene slope incisions off New Jersey: Are they diagnostic of sequence
632 boundaries?. Geology. 112, 817-828.

633

634 Gély, J-P., Sztràkos, K., 2000. L‘évolution paléogéographique et géodynamique du
635 Bassin aquitain au Paléogène : enregistrement et datation de la tectonique pyrénéenne.
636 Géologie de la France. 2000-2, 31–57.

637

638 Gély, J-P., Sztràkos, K., 2001. La tectonique pyrénéenne à l‘Oligocène : une phase
639 majeure de déformation en compression méconnue du Bassin aquitain (France).
640 Comptes Rendus de l‘Académie des Sciences, Paris. 332, 507–512.

641

642 Guillocheau, F., Bonnet, S., Bourquin, S., Dabard, M-P., Outin, J-M., Thomas, E.,
643 1998. Mise en évidence d‘un réseau de paléovallées ennoyées (paléorias) dans le
644 Massif armoricain: une nouvelle interprétation des sables pliocènes armoricains.
645 Comptes Rendus de l‘Académie des Sciences, Paris. 327, 237– 243.

646

647 Guillocheau, F., Robin, C., Allemand, P., Bourquin, S., Brault, N., Dromart, G.,
648 Friedenberg, R., Garcia, J-P., Gaulier, J-M., Gaumet, F., Grosdoy, B., Hanot, F., Le
649 Strat, P., Mettraux, M., Nalpas, T., Prijac, C., Rigollet, C., Serrano, O., Granjean, G.,
650 2000. Meso-Cenozoic geodynamic evolution of the Paris Basin : 3D stratigraphic
651 constraints. Geodynamica Acta. 13, 189-246.

652

653 Guillocheau F., Brault N., Thomas E., Barbarand J., Bonnet S., Bourquin S., Estéoule-
654 Choux J., Guennoc P., Menier D., Néraudeau D., Proust J-N., Wyns R., 2003. Histoire

géologique du Massif Armoricain depuis 140Ma (Crétacé-Actuel). Bulletin d'Information des Géologues du Bassin de Paris. 40, 13-28.

Hailwood, E.A., Bock, W., Costa, L., Dupeuble, P.A., Müller, C., Schnitker, D., 1979. Chronology and biostratigraphy of northeast Atlantic sediments, DSDP Leg 48. In: Montardet, L., Roberts, D.G., et al. (Eds.), Initial Report of the Deep Sea Drilling Project. Washington. 1119-1141.

Haq, B.U., Hardenbol, J., Vail, P.R., 1987. Chronology of fluctuatingsea levels since the Triassic. Science. 235, 1156– 1167.

Haq, B.U., Hardenbol, J., Vail, P.R., 1988. Mesozoic Cenozoic chronostratigraphy and eustatic cycles. In: Wilgus, C.K., Posamentier, H., Ross, C.K., Kendall, C.G.St.C. (Eds.), Sea-level Changes: An Integrated Approach. Society of Economic Paleontologists and Mineralogists Special Publication. 42, 71–108.

Hilgen, F., Aziz, H.A., Bice, D., Iaccarino, S., Krijgsman, W., Kuiper, K., Montanari, A., Raffi, I., Turco, E., Zachariasse W.-J., 2005. The Global boundary Stratotype Section and Point (GSSP) of the Tortonian Stage (Upper Miocene) at Monte Dei Corvi. Episodes. 28, 6-17.

676 Imbrie, J., Hays, J.D., Martinson, D.G., McIntyre, A., Mix, A.C., Morley, J.J., Pisias,
677 N.G., Prell, W.L., Shackleton, N.J., 1984. The orbital theory of Pleistocene climate:
678 support from a revised chronology of the marine δ 18O record. In: Berger A, Imbrie J,
679 Hays J, Kukla G, Saltzman B. (Eds.), Milankovitch and climate. Reidel Publishing
680 Company, Dordrecht, 269-305.

681

682 John, C.M, Karner, G.D., Mutti, M., 2004. $\delta^{18}O$ and Marion Plateau backstripping:
683 Combining two approaches to constrain late middle Miocene eustatic amplitude.
684 Geology. 32, 829-832.

685

686 Kominz, M.A., Miller, K.G., Browning, J.V., 1998. Long-term and short-term global
687 Cenozoic sea-level estimates. Geology. 26, 311–314.

688

689 Lécuyer, C., Grandjean, P., Paris, F., Robardet, M., Robineau, D., 1996. Deciphering
690 « temperature » and « salinity » from biogenic phosphates : the ^{18}O of coexisting
691 fishes and mammals of the Middle Miocene sea of western France. Paleogeography,
692 Paleoclimatology, Paleoecology. 126, 61-74.

693

694 Lericolais G., Auffret J-P. Bourillet J-F., 2003. The Quaternary Channel River :
695 seismic stratigraphy of its palaeo-valleys and deeps. Journal of Quaternary Science.
696 18, 245-260.

697

698 Lofi, J., and Berné, S., 2008. Evidence for pre-Messinian submarine canyons on the
699 Gulf of Lions slope (Western Mediterranean). Marine and Petroleum Geology. 25,
700 804-817.

701

702 Lofthouse, C., Robert, A., 2008. Riffle-pool sequences and meander morphology.
703 Geomorphology. 99, 214-223.

704

705 Maillard, J., 1982. Rapport de fin de sondage Garlizenn-1 (GEN 1), Mer Celtique
706 permit, S.N.E.A.P. (Société National Elf Aquitaine Production). BEPH (Bureau
707 Exploration-Production des Hydrocarbures) Open file report 14-3527. 20 pp.

708

709 Menier, D., 2004. Morphologie et remplissage des vallées fossiles sud-armoricaines:
710 apports de la stratigraphie sismique. Ph.D. Thesis memoir, Université de Bretagne
711 Sud, Mémoires Géosciences Rennes. 110, 202 pp.

712

713 Menier, D., Reynaud, J-Y., Proust, J-N., Guillocheau, F., Guennoc, P., Bonnet, S.,
714 Tessier, B., Goubert, E., 2006. Basement control on shaping and infilling of valleys
715 incised at the southern coast of Brittany, France. Society of Economic Paleontologists
716 and Mineralogists Special Publication. 85, 37-55.

717

718 Miller, K.G., Mountain, G.S., Browning, J.V., Kominz, M., Sugarman, P.J., Christie-
719 Blick, N., Katz, M. E., Wright, J.D., 1998. Cenozoic global sea level, sequences, and

720 the New Jersey Transect: results from coastal plain and continental slope drilling.
721 Reviews of Geophysics. 36, 569-601.

722

723 Miller, K.G., Kominz, M., Browning, J.V., Wright, J.D., Mountain, G.S., Katz, M.E.,
724 Sugarman, P.J., Cramer, B.S., Christie-Blick, N., Pekar, S.F., 2005. The Phanerozoic
725 record of sea-level change. Science. 310, 1293-1298.

726

727 Miller, K.G. Browning, J.V., Aubry, M-P., Wade, B.S., Katz, M.E., Kulpecz, A.A.,
728 Wright, J.D., 2008. Eocene-Oligocene global climate and sea-level changes: St.
729 Stephens Quarry, Alabama. Geological Society of America Bulletin. 120, 34-53.

730

731 Montadert L., Roberts D.G., De Charpal O., Guennoc P., 1979. Rifting and
732 subsidence of the northern continental margin of the Bay of Biscay. in : Usher X.
733 (Ed.), Initial Reports of the Deep Sea Drilling Project, Washington. 48, 1025–1060.

734

735 Néraudeau, D., 2003. Lithologies, Faunes et Paléogéographies des Dépôts de Type
736 Falun. Bulletin d'Information des Géologues du Bassin de Paris. 40, 6-12.

737

738 Olivet J-L., 1996. La cinématique de la plaque Ibérique. Bulletin des Centres de
739 Recherche, d'Exploration et de Production d'Elf- Aquitaine. 21, 131–195.

740

741 Pigram, C.J., Davies, P.J., Feary, D.A., Symonds, P.A., 1992. Absolute magnitude of
742 the second-order middle to late Miocene sea-level fall, Marion Plateau, Northeast
743 Australia. Geology. 20, 858-862.

744

745 Pinot, J-P., 1974. Le Précontinent Breton entre Penmac'h, Belle-Ile et l'escarpement
746 continental, Etude Géomorphologique, Lannion, Impram, 256 pp.

747

748 Posamentier, H.W., 2001. Lowstand alluvial bypass systems: incised vs. unincised.
749 American Association of Petroleum Geologists Bulletin. 85, 1771-1793.

750

751 Posamentier, H.W., P.R. Vail, 1988. Eustatic controls on clastic deposition II—
752 sequence and systems tract models. In*:* C. K. Wilgus, B. S. Hastings, C. G. St. C.
753 Kendall, H. W. Posamentier, C. A. Ross, J. C. Van Wagoner, eds., Sea level change—
754 an integrated approach: Society of Economic Paleontologists and Mineralogists
755 Special Publication. 42, 125–154.

756

757 Powell, A.J., 1988. A preliminary investigation into the Neogene dinoflagellate cyst
758 biostratigraphy of the British Southwestern Approaches. Bulletin des Centres de
759 Recherche, Exploration et Production Elf-Aquitaine. 12, 277–311.

760

761 Praeg, D., Stokerb, M.S., Shannona, P.M., Ceramicolac, S., Hjelstuend, B., Laberge,
762 J.S., Mathiesenf A., 2005. Episodic Cenozoic tectonism and the development of the

763 NW European ‗passive' continental margin. Marine and Petroleum Geology. 22,
764 1007–1030.

765

766 Preux, R.,1978. Rapport de fin de sondage Penma-1, Loire Maritime permit,
767 S.N.E.A.P. (Société National Elf Aquitaine Production). BEPH (Bureau Exploration-
768 Production des Hydrocarbures) Open file report 14-3435. 15 pp.

769

770 Proust, J-N., Renault, M., Guennoc, P., Thinon, I., 2009. Sedimentary architecture of
771 the Loire drowned valleys of the French Atlantic shelf. Journal of Sedimentary
772 Research. In press.

773

774 Reynaud, J-Y., Tessier, B., Proust, J.N., Dalrymple, R., Bourillet, J-F., De Batist, M.,
775 Lericolais, G., Berné, S. Marsset, T., 1999. Architecture and sequence stratigraphy of a
776 late neogene incised valley at the shelf margin, Southern Celtic Sea. Journal of
777 Sedimentary Research, 69, 351-364.

778

779 Richards, K.S., 1982. Rivers: Form and Process in Alluvial Channels: New York,
780 Methuen, 361 pp.

781

782 Stewart, H.A., Davies, J.S., 2007. SW Approaches MESH Survey, R/V Celtic
783 Explorer Cruise CE0705, BGS Project 07/06, Operations Report. British Geological
784 Survey Commissioned Report, CR/07/123.

785

786 Tcherepanov, E.N., Droxler, A.W., Lapointe, P., Mohn, K., 2008. Carbonate seismic
787 stratigraphy of the Gulf of Papua mixed depositional system: Neogene stratigraphic
788 signature and eustatic control. Basin Research. 20, 185-209.

789

790 Thinon, I., 1999. Structure profonde de la Marge Nord Gascogne et du Bassin
791 Armoricain. Ph.D. Thesis memoir, Université de Bretagne Occidentale.

792

793 Thinon, I., Menier, D., Guennoc, P., Proust, J-N., Guillocheau, F., Bonnet, S., Le Roy,
794 P., Augris, C., Bourillet, J-F., Baltzer, A., Tessier, B., Pastol, Y., Garlan, T.,
795 Bechennec, F., Le Metour, J., Graviou, P., Alix, A.S., Cornu, S., Loget, N., Scalliet,
796 F., 2008. Carte géologique de la France à 1 / 250 000 de la marge continentale,
797 Lorient, Bretagne Sud. Éditions BRGM-CNRS.

798

799 Thomas, E., 1999. Évolution Cénozoïque d'un domaine de socle : le Massif
800 Armoricain. Ph.D. unpublished Thesis memoir, Université de Rennes 1. 148 p.

801

802 Vail, P.R., Mitchum, J.R., Todd, R.G., Widmier, J.M., Thompson, S., Sangree, J.B.,
803 Bubb, J.N., Hatlelid, W.G., 1977. Seismic stratigraphy and global changes of sea level
804 in depositional sequences. In *Seismic Stratigraphy – applications to hydrocarbon*
805 *exploration*, Payton, E. (Ed): American Association of Petroleum Geologist Memoir.
806 26, 49-212.

807

808 Vail, P. R., Audemard, F., Bowman, S. A., Eisner, P. N., Perez-Cruz, C., 1991. The
809 stratigraphic signatures of tectonics, eustasy and sedimentology—An overview, in*:*
810 Einsele, G., et al., eds., Cycles and events in stratigraphy: Berlin, Springer-Verlag.
811 617–659.

812

813 Vanney J. R., Horn R., Martin G., 1972. La disposition des séquences sédimentaires
814 post-mésozoïques sous la partie externe de la plate-forme continentale sud-
815 armoricaine (entre 45°40‘ et 46°40‘ lat. Nord). Compte Rendus de l‘Académie des
816 Sciences. 275, 2829-2832.

817

818 Van Vliet-Lanoë, B., Laurent, M., Hallégouët, B., Margerel, J-P., Chauvel, J-J.,
819 Michel, Y., Moguedet, G., Trautman, F., Vauthier, S., 1998. Le Mio–Pliocène du
820 Massif armoricain. Données nouvelles. Comptes Rendus de l‘Académie des Sciences,
821 Paris. 326, 333–340.

822

823 Waelbroeck, C. Labeyrie, L., Michel, E., Duplessy, J-C., McManus, J.F., Lambeck,
824 K., Balbon, E., Labracherie, M, 2002. Sea-level and deep water temperature changes
825 derived from benthic foraminifera isotopic records. Quaternary Science Reviews. 21,
826 295-305.

827

828 Zachos, J., Pagani, M., Sloan, L., Thomas, E., Billups, K., 2001. Trends, rhythms, and
829 aberrations in global climate 65 Ma to present. Science. 292, 686-693.

830

831 Ziegler, P.A., 1987. Evolution of the Western Approaches Trough. Tectonophysics,
832 137, 341-346.

833

834 Ziegler, P.A., 1990. Collision related intra-plate compression deformations in western
835 and central Europe. Journal of Geodynamic. 11, 357-388.

836

837 **FIGURE CAPTIONS:**

838

839 **Figure 1:** A- Map showing the location of the study area in the Bay of Biscay, W.A.:
840 Western Approaches, A.S.: Armorican Shelf, Aq.S.: Aquitaine Shelf; B – Simplified
841 geological map covering the Armorican Shelf, showing the extent of the main
842 geological units and the position of exploration well and offshore cores with retrieved
843 Cenozoic material (Andreieff et al., 1968; Barbaroux et al., 1971; Bouysse et al.,
844 1974; Delanoë and Pinot, 1974; Delanoë et al., 1975; Delanoë et al., 1976). Thin
845 dashed lines correspond to the position of geophysical data (see fig. 2 for details). The
846 Bold lines correspond to the profiles displayed on figure 3; C – Cross section of the
847 Armorican Shelf showing the main stratigraphic succession from Cretaceous to
848 present. The vertical axis is in second two-way travel time (TWTT) (modified from

849 Vanney et al., 1972; Guillocheau et al., 2003, Thinon et al., 2008). See Fig. 1B for
850 location.

851

852 **Figure 2:** Position maps showing the extension of the four Sparker-type seismic
853 surveys (Bir Hacheim 1967; Trophal 2002; GeoEtel 2008) used in this study,
854 including line numbers and the sections displayed in figures (bold lines).

855

856 **Figure 3:** Lithological section of PENMA-1 exploration well with lithology
857 description, biostratigraphy correlations established from foraminifer and nannofossil
858 determinations, and interpretation of depositional environments (adapted from Preux,
859 1978). Top Oligocene and intra Oligocene labels mark two important changes in the
860 depositional environment settings that may correlate to seismic unconformities.

861

862 **Figure 4:** Interpreted seismic profiles from BH67 (20-670; 20-790; 20-970) and
863 GeoEtel 2008 (A) surveys showing the stacking pattern of the main seismic units (U1
864 to U6b) and unconformities (S1 to S6) from the inner shelf to the shelf break. On
865 profile 20-670, seismic units and unconformities are correlated to the calculated
866 position of top- and intra-Oligocene markers in projected PENMA-1 (c. 3 km from
867 NW). The box on profile GeoEtel-2008 A refers to the section displayed in figure 4a.

868

869 **Figure 5:** Seismic image and interpreted section of Sparker seismic profiles GeoEtel-
870 07 (A) and Job 1974 (3-VIII-74) (B) (see Figure 1 for location) showing the

interpreted seismic units (U2 to U6b) and unconformities (S2 to S6). Three buried incised valleys are identified on S4 and labeled A, B and C. Valley B is displayed in detail in figure 6 as indicated by boxes. See figures 2 and 4 for Location of profiles. Note that the zoom on Fig. 6a. is a crop of GeoEtel 2008 – 26 but is indicated by a box on Job 1974 (3-VIII-74) as both profiles are similar in location.

Figure 6: Details of high-resolution Sparker profiles from GeoEtel-2008 survey crossing the incised fluvial valleys of S4 (valley B), from profiles 26 (A), 22 (B) and 07 (C). Profiles show the main incision channel (MC) and associated tributaries (Tr) separated by terraces (Te) in a wider valley. On profile 07 (C) other younger channelized incisions (YCI) are visible that cut the major erosion surface S4. Vertical axis in ms (TWTT: Two Way Travel Time) and horizontal axis shows Shot Point number (SP). See Figs. 1 and 3 for location.

Figure 7: Oblique three-dimensional view from North showing the interpreted seismic profiles GeoEtel 07, 21, 22, 25 to 29 and Trophal 50 (labels) and the fluvial incisions developed on the major erosion surface S4 (bolder line). The dotted lines correspond to proposed reconstructions of the incised valleys B and C. Vertical axis in ms (TWTT: Two Way Travel Time) and horizontal axis shows Shot Point number (SP).

Figure 8: Map of the Armorican Shelf showing (1) the cartographic trace of S4 within the Miocene series, (2) the reconstruction of the buried fluvial network with

894 the four valleys (A, B, C and D), (3) the mid-Miocene (Serravallian-Tortonian) fluvial
895 remnants identified onshore at Lauzach and Réguigny (Brault et al., 2004), and (4) the
896 ~~–~~Quaternary incised valleys" (Menier, 2004; Menier et al., 2006; Thinon et al., 2008) .
897 The Pleistocene incised fluvial network is preserved offshore until -70 m where
898 incision starts to fade over the mid-shelf (Menier et al., 2006). Direct connection
899 between networks is precluded by erosion onshore and by the major erosion surface
900 S6 of the AS offshore.

901

902 **Figure 9:** Correlation of the AS seismic stratigraphy to (1) the Western Approaches
903 seismic stratigraphy (*e.g.* Bourillet et al., 2003), (2) the onshore fluvial stratigraphy
904 (Van Vliet-Lanoë et al., 1997, Guillocheau et al., 1998; Brault et al., 2004), (3) the
905 PENMA-1 section (Preux, 1978), (4) the global sea level curve (modified from Haq et
906 al., 1987), (5) the main orogenic phases affecting the western Europe, and (6) the
907 Stratigraphic chart (ICS, 2008).

908

909 Table 1: Characteristics of the seismic units (U1 to U6b) and bounding surfaces (S1 to
910 S6) recognized on the data covering the AS with seismic description, Lithological
911 interpretation and examples from GeoEtel-2008 survey.

912

Figure 1

Click here to download high resolution image

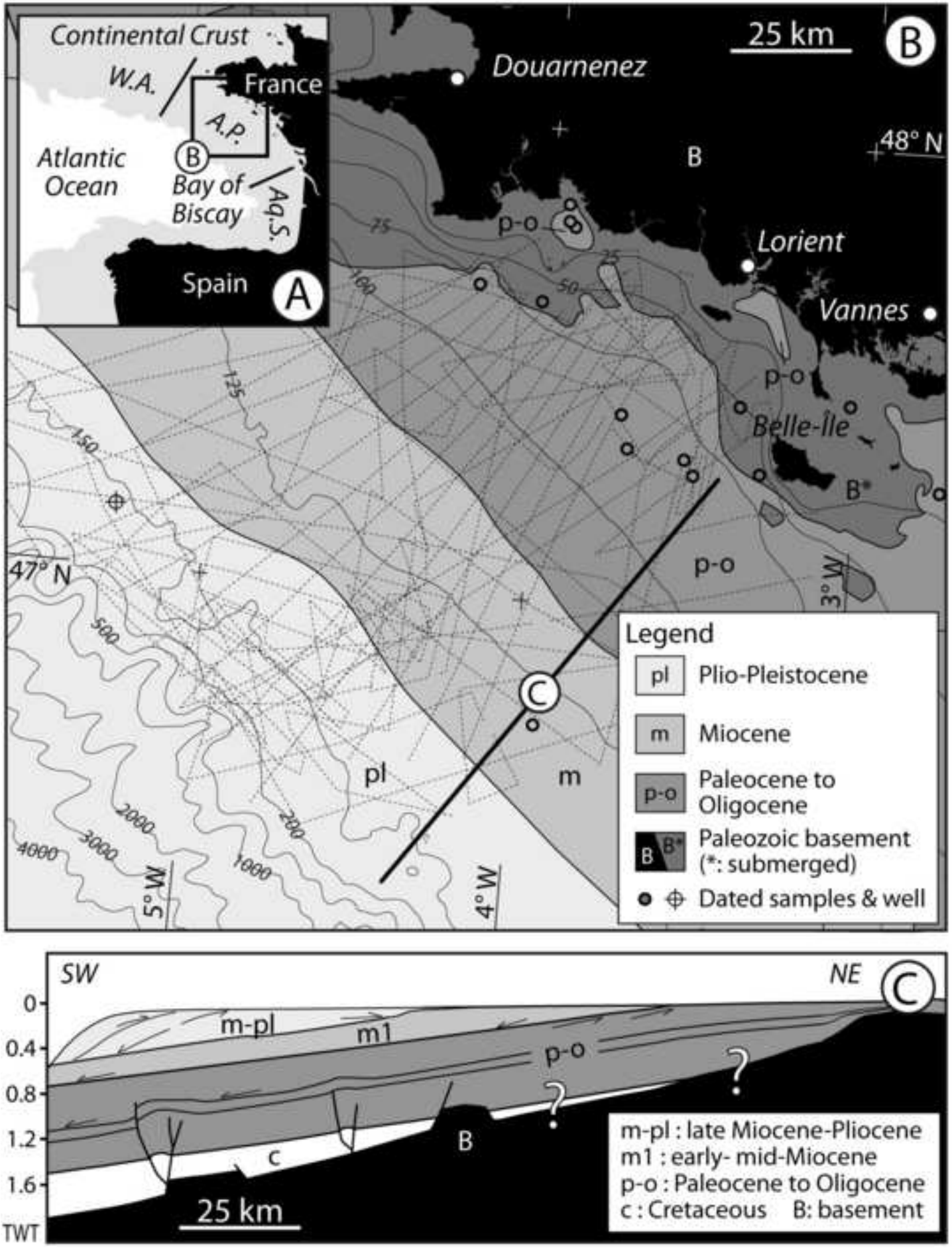

Figure 2

Click here to download high resolution image

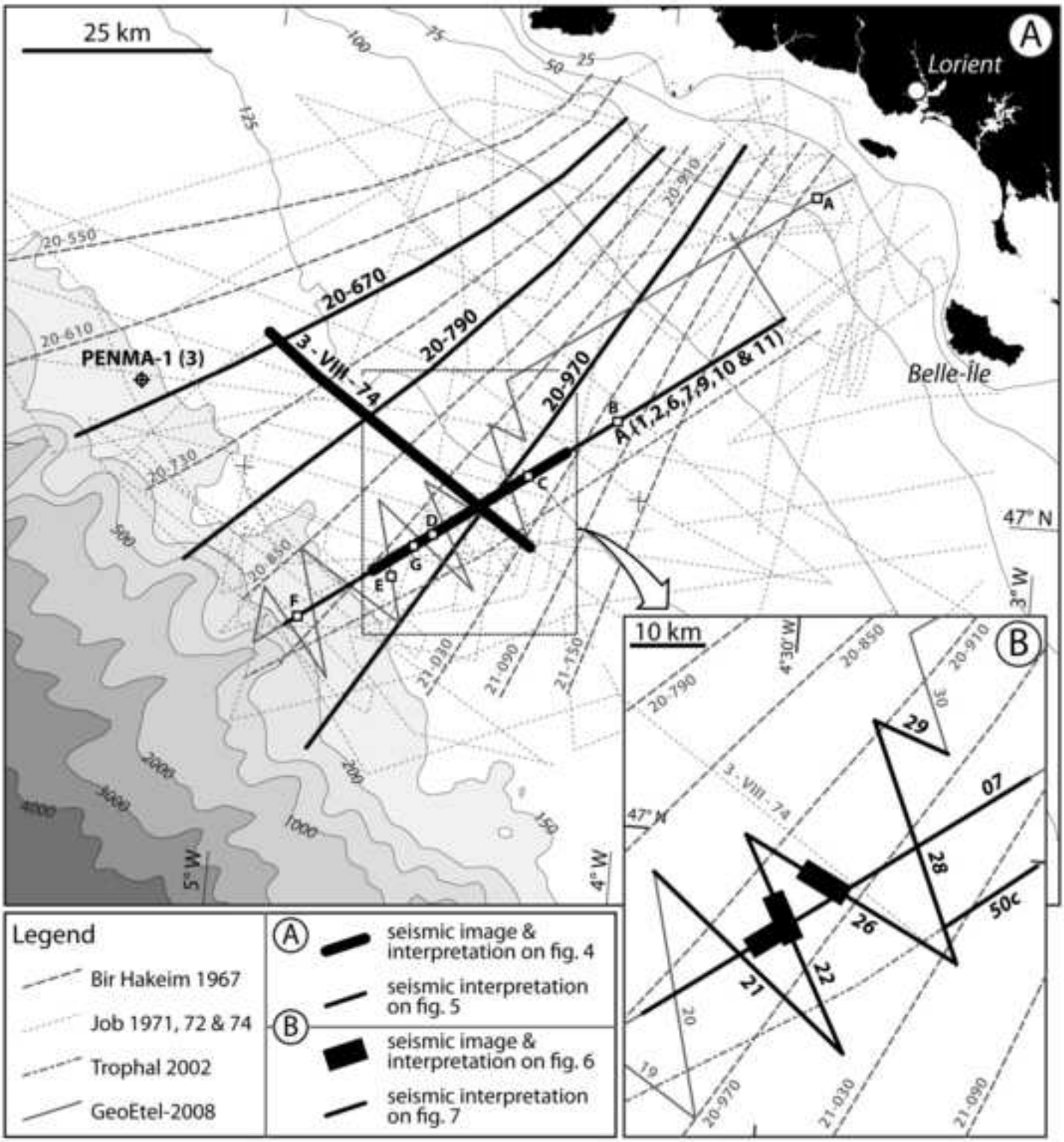

Figure 3

Click here to download high resolution image

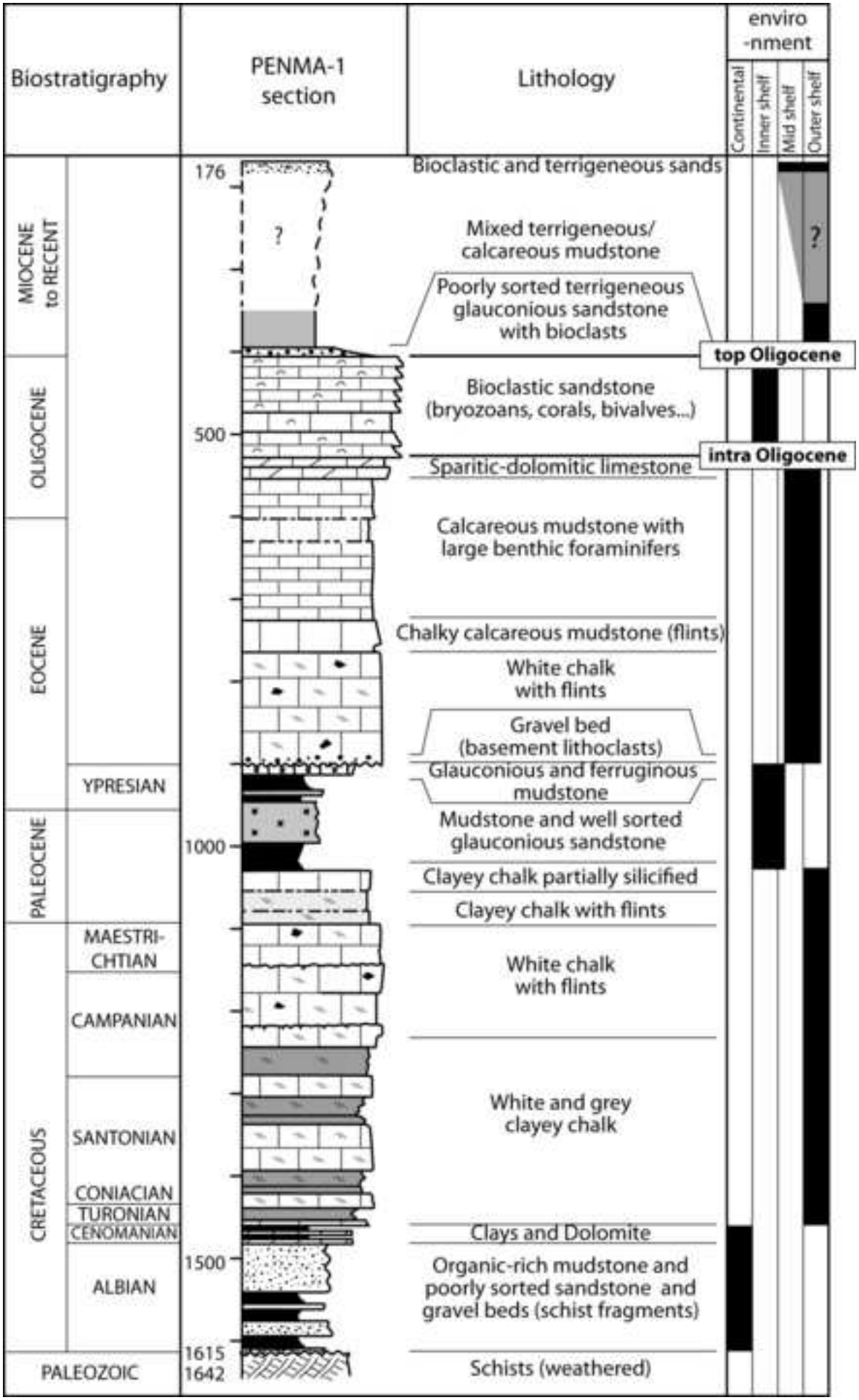

Figure 4

Click here to download high resolution image

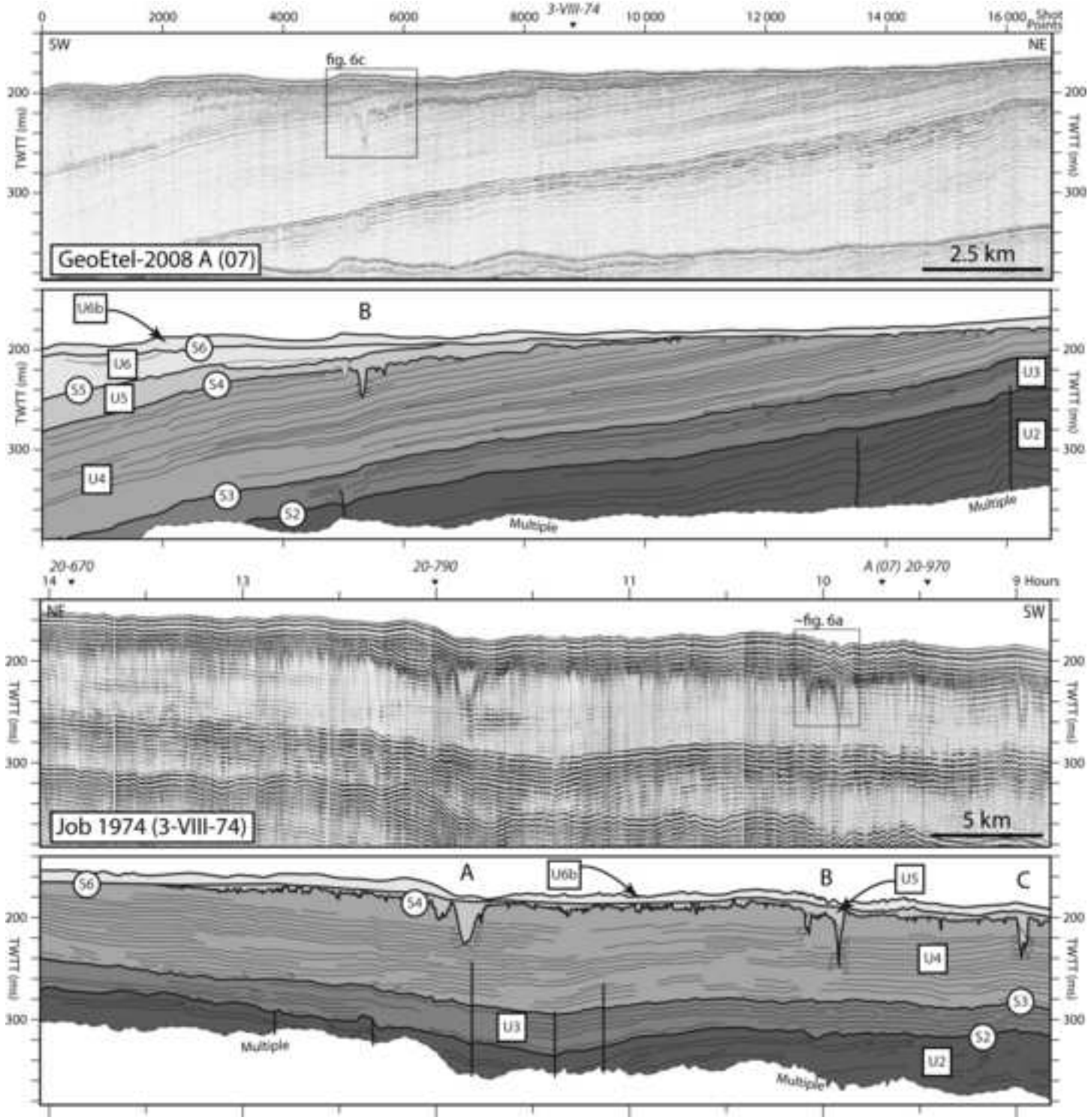

Table 1

Click here to download high resolution image

Seismic units	Descriptions of seismic facies & reflection terminations	Interpretations / correlations	Seismic image samples (crops from GeoEtel-2008) Scale bars: horizontal – 250 m ; vertical = 20 ms
U1	Very low to average continuity, high amplitude and frequency, subparallel to chaotic configuration. Highly deformed **Base**: not determined **Top**: eroded by S1 (top lap)	Crystalline and metamorphic basement (Paleozoic)	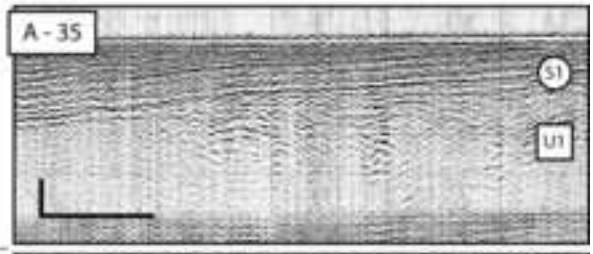
U2	Good continuity, average frequency, average to high amplitude, parallel configuration. Faulted & folded **Base**: onlap on S1 **Top**: eroded by S2 (toplap)	Well-bedded marine deposits identified as Paleocene and Eocene chalky calcareous mudstones in various cores and in PENMA-1 well	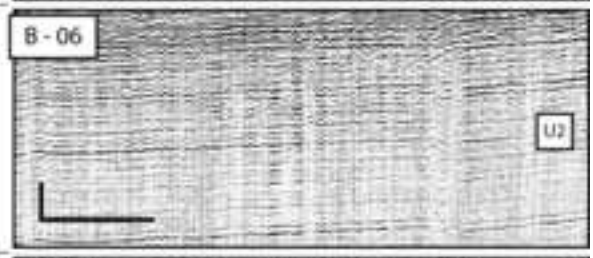
U3	Average continuity, average frequency, very high amplitude, subparallel to wavy configuration. Slightly faulted & folded **Base**: concordant on S2 **Top**: concordant with S3	Bedded marine deposits with mounds (coral patches?) correlated to Oligocene bioclastic sandstones with corals, bivalves and bryozoans in PENMA-1 well	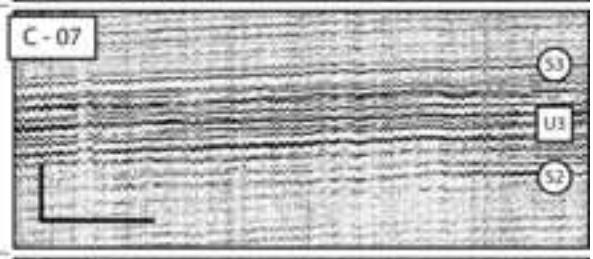
U4	Good continuity, average frequency, low amplitude, subparallel configuration with clinoforms. Rarely faulted & folded **Base**: downlap on S3 **Top**: eroded by S4 with incisions	Well-bedded marine deposits corresponding to mixt terrigeneous / calcareous Miocene mudstones in core samples and PENMA-1 well	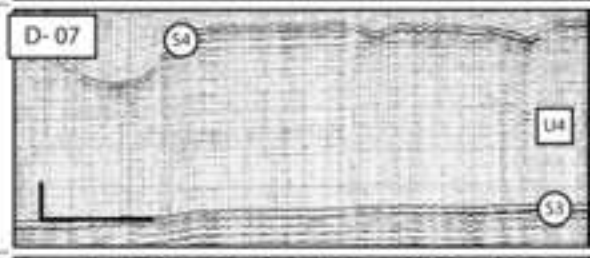
U5	Very low continuity, average frequency, very low amplitude, chaotic configuration with channels. Rarely faulted & folded **Base**: onlap on S4 **Top**: eroded upward and downward by S5 with incisions	Pourly-bedded coarse marine and channel fill (fluvial) LST deposits of probable Late Miocene age.	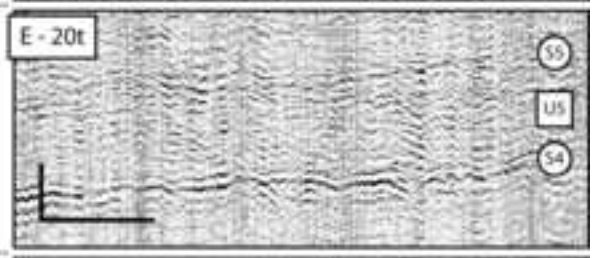
U6	Very low continuity, average frequency, low amplitude, chaotic configuration with channels & clinoforms. Rarely faulted & folded **Base**: concordant/onlap on S5 **Top**: eroded by S6 (toplap)	Pourly-bedded coarse marine deposits with rare channels corresponding to the outer-shelf Pliocene - Pleistocene sediment wedge (Red sands)	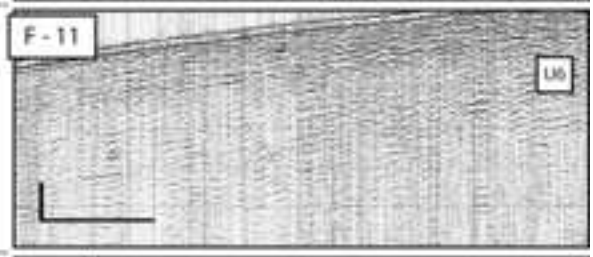
U6b	Transparent to low continuity, low amplitude. Not deformed **Base**: concordant/downlap on S6 **Top**: sea floor	Poorly-bedded muddy sands of disconnected sediment bodies of the Pleistocene - Holocene "Grande Vasière", deposited and reworked during LST and/or TST	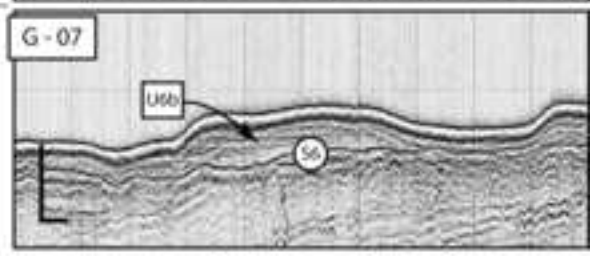

Figure 5

Click here to download high resolution image

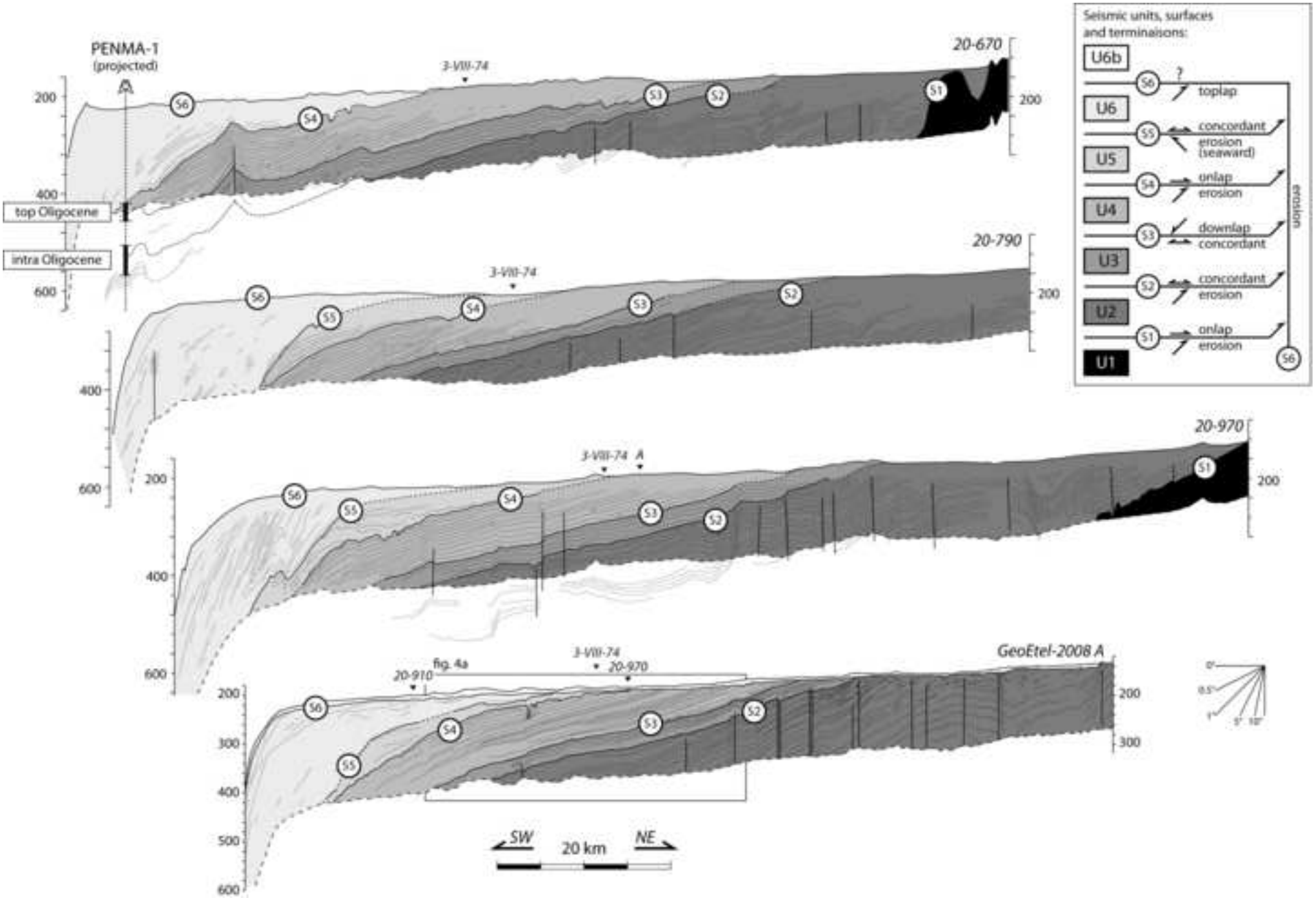

Figure 6

Click here to download high resolution image

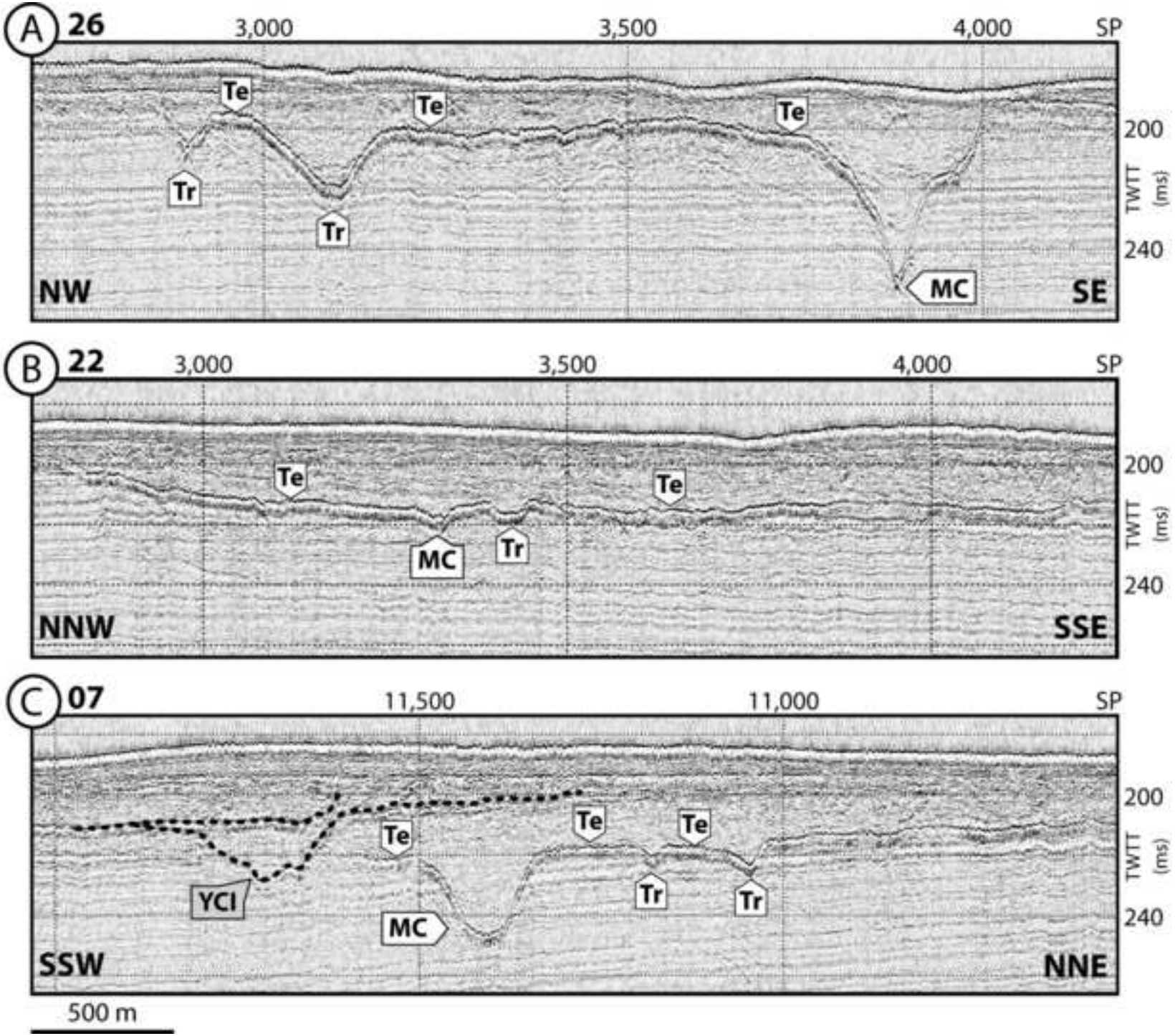

Figure 7

Click here to download high resolution image

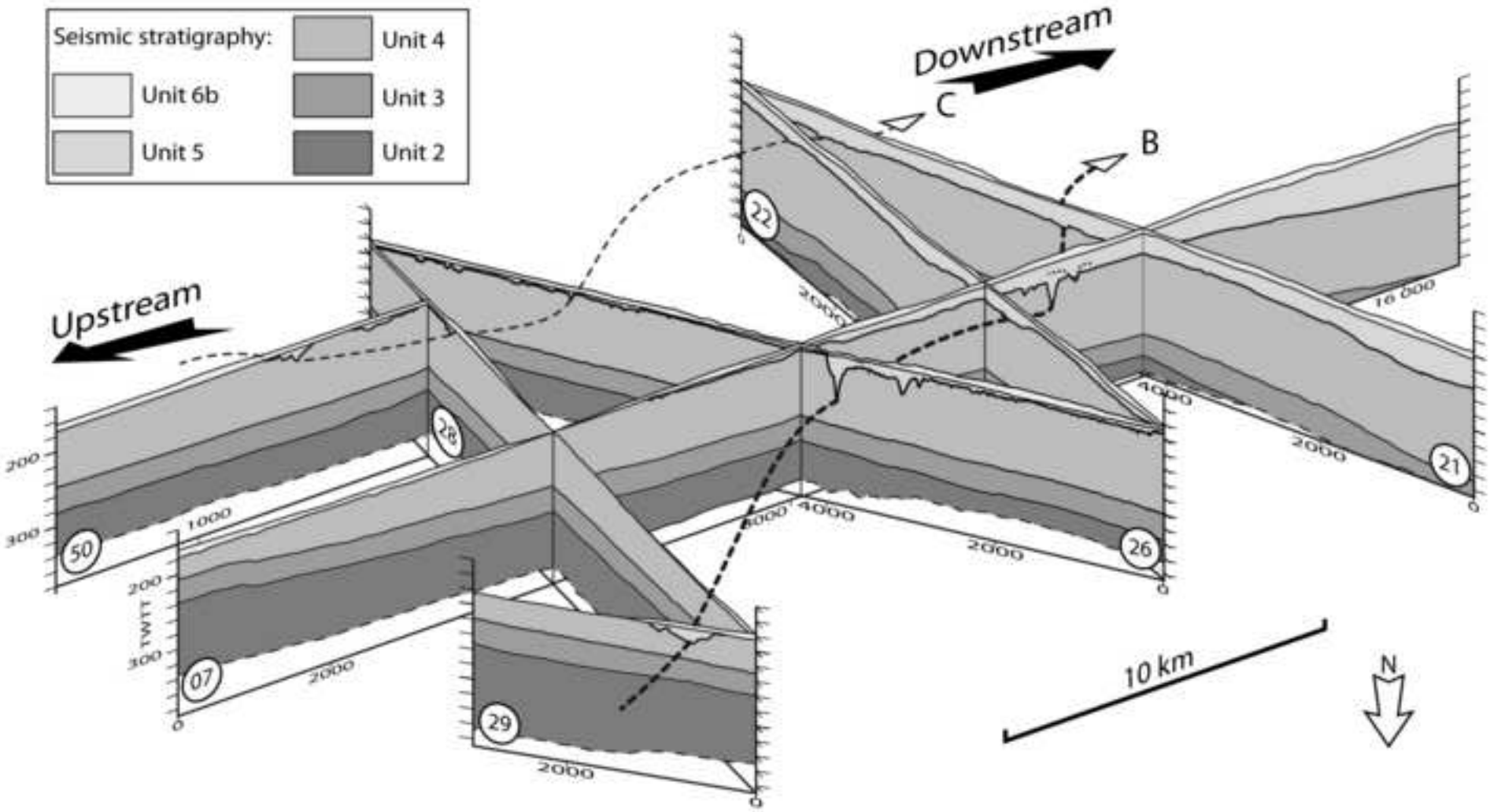

Figure 8

Click here to download high resolution image

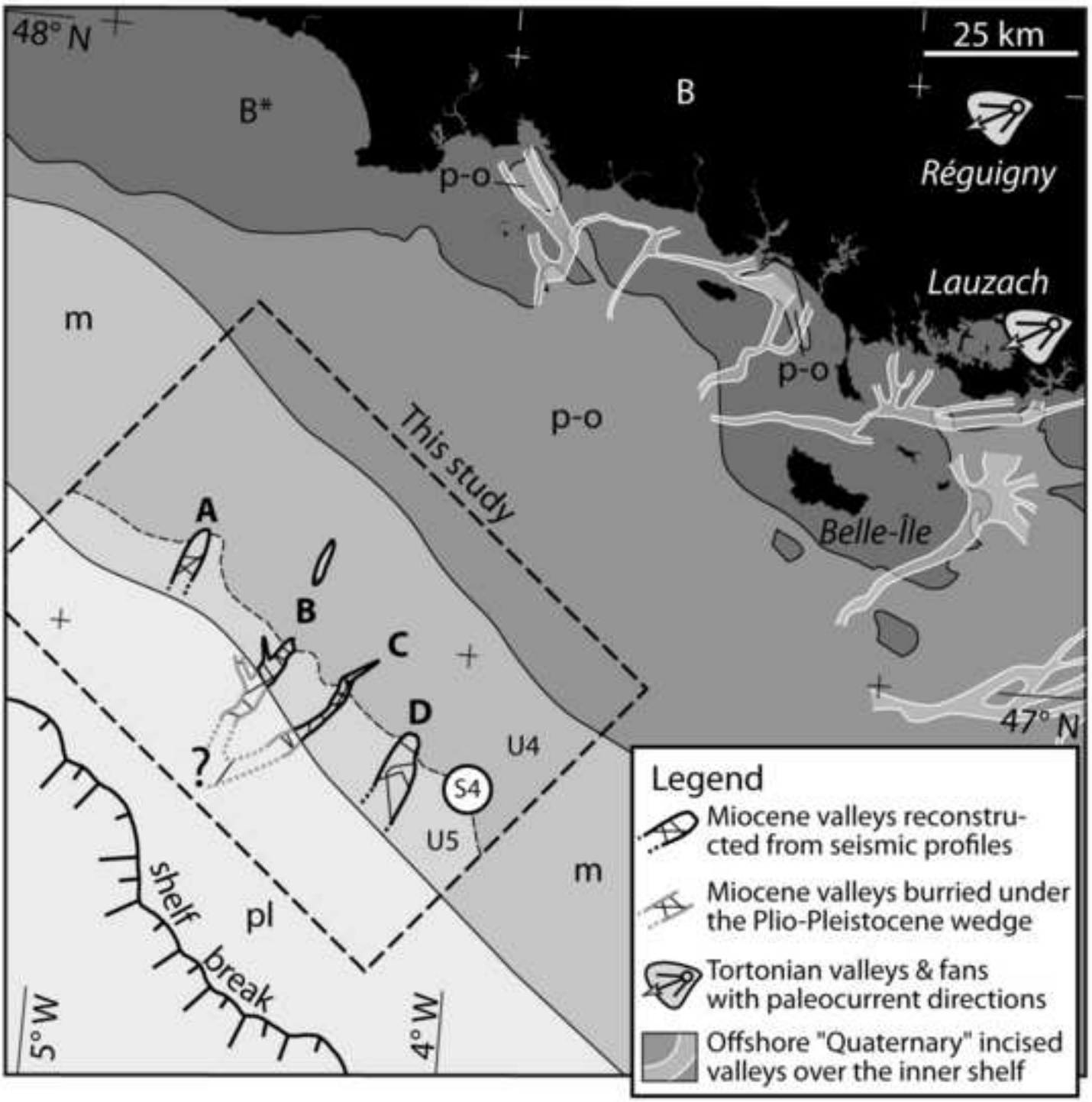

Figure 9

Click here to download high resolution image